

# Structural, Electronic, and Magnetic Properties of $\text{Co}_n(\text{benzene})_m$ Complexes

Xiuyun Zhang and Jinlan Wang\*

Department of Physics, Southeast University, Nanjing 211189, P. R. China

Received: August 18, 2007; In Final Form: October 8, 2007

The structural, electronic, and magnetic properties of cobalt–benzene complexes ( $\text{Co}_n\text{Bz}_m$ ,  $n, m = 1-4$ ,  $m = n, n + 1$ ) have been explored within the framework of an all electron gradient-corrected density functional theory. Sandwich conformations are energetically preferred for the smallest series of  $n, m = 1-2$ , rice-ball structures are for larger sizes with  $n \geq 3$ , and both motifs coexist for  $\text{Co}_2\text{Bz}_3$ . The rice-ball clusters of (3, 3) and (4, 4) are more stable than (3, 4) having a relative large binding energy and HOMO–LUMO gap whereas smaller sandwich clusters have highly kinetic stability at  $(n, n + 1)$ . The computed ionization potentials and magnetic moments of  $\text{Co}_n\text{Bz}_m$  are in good agreement with the measured values overall; the present results suggest that the measured moments are averages reflecting mixtures of a few nearly isoenergetic isomers having different spin states. The magnetism of the complexes mainly comes from Co atoms with a Bz molecule only possessing very small moments. Ferromagnetic ordering is energetically preferred for smaller complexes with  $n = 1-3$  whereas antiferromagnetic ordering is favored for (4, 4). The relatively smaller moments of  $\text{Co}_n$  clusters in a Bz matrix indicate that Bz molecules play an attenuation role to the magnetism of the complexes.

## I. Introduction

Metal–ligand complexes exhibit rich structures and physical and chemical properties, and they have been extensively studied because of their potential applications in catalysis, polymers, and molecular recognition, to name a few.<sup>1</sup> Complexes comprised of transition metal atoms and benzene molecule are one of the most active areas, and a number of experimental and theoretical explorations of their geometric, energetic, electronic, magnetic, and optical properties have been made.<sup>2–36</sup> One of more interesting findings is that the structures of the complexes depend on the identify of the metal elements: linearly multidecked sandwich clusters are formed for early transition metal Sc, Ti, and V and “rice-ball” conformations are preferred for late transition metals Fe, Co, and Ni.<sup>2,3,26–32</sup> Recently, the combined use of Stern–Gerlach molecular beam deflection experiments and density functional theory (DFT) computations have revealed magnetic nature of multidecked vanadium- $n$ -benzene $_{n+1}$  ( $\text{V}_n\text{Bz}_{n+1}$ ) sandwich clusters.<sup>24–30</sup>

Compared to the substantial effort applied to understanding vanadium-benzene complexes, there have been relatively few studies of the late transition metal-benzene complexes such as cobalt-benzene ( $\text{Co-Bz}$ ,  $\text{Bz} = \text{C}_6\text{H}_6$ ).<sup>2–16</sup> Kurikawa et al.<sup>2,3</sup> have synthesized  $\text{Co}_n\text{Bz}_m$  clusters by the reaction of laser-vaporized Co atoms with benzene vapor and found that stable compositions are formed at  $(n, m) = (1, 2), (2, 3), (3, 3), (4, 4), (5, 4), (6, 4), (7, 4), (8, 5), (9, 6)$ ; they have also inferred that the structures depend on the compositions: sandwich structures are suggested for small sizes of  $n = 1-2$ ,  $m = n + 1$ ; rice-ball structures are for  $n \geq 3$ ; both sandwich and rice-ball structures coexist for (2, 3). However, Gerhards et al.<sup>5</sup> have proposed that cobalt–benzene anionic clusters are sandwich structures for the sizes with  $n = 1-3$ ,  $m = n, n + 1$  based on photoelectron spectroscopy (PES) studies. Rayane et al.<sup>11</sup> have measured the

permanent electric dipole moment of  $\text{CoBz}_2$  and determined that it possesses an asymmetric structure. Bechamp et al.<sup>6</sup> have characterized  $\text{CoBz}$  and  $\text{CoBz}_2$  complexes using infrared spectroscopy (IR) and electron paramagnetic resonance (EPR), and these studies suggest the low-symmetry structures for these complexes. Jaeger et al.<sup>7</sup> have identified that  $\text{CoBz}^+$  possesses  $C_{2v}$  structure and  $\text{CoBz}_2^+$  has a  $D_{6h}$  or  $D_{6d}$  symmetry by combining IR spectroscopy and DFT computations. On the basis of Stern–Gerlach molecular beam deflection studies, Knickelkein<sup>8</sup> has postulated sandwich-like clusters with sizes of  $n = 2-4$  based on their relatively high magnetic moments and core–shell clusters for  $n = 4-10$ , which, in contrast, display relatively low moments, due to quenching of the underlying polynuclear Co cluster by the adsorbed overlayer of benzene.

On the other hand, theoretical studies on  $\text{Co}_n\text{Bz}_m$  complexes are scarce and most are limited to the smallest complexes of  $\text{CoBz}$  and  $\text{CoBz}_2$ .<sup>9–15</sup> Chaquin et al.<sup>9</sup> have performed DFT computations on the structures and electronic properties of neutral and cationic  $\text{CoBz}$ . Bauschlicher et al.<sup>10</sup> have carried out a modified coupled pair functional method on cationic  $\text{CoBz}$ . Pandey et al.<sup>13</sup> have explored the equilibrium geometry, dissociation energy, electronic structure, and magnetic properties of neutral, cationic, and anionic  $\text{CoBz}$  and  $\text{CoBz}_2$  complexes using PW91/DNP approach. Zhou et al.<sup>15</sup> have determined  $\text{Co}_2\text{-Bz}_2$  is a coaxial  $D_{6h}$  structure with two cobalt atoms sitting on a line and perpendicular to the benzene plane computationally. For the clusters larger than (2, 2), there is no theoretical report available yet. Therefore, it is very necessary to extend the study to larger sizes to identify the structures (sandwich or rice-ball) and provide theoretical explanations of their novel magnetic properties of  $\text{Co}_n\text{Bz}_m$  complexes.

In this Article, we systematically study the structural, electronic, and magnetic properties of neutral  $\text{Co}_n\text{Bz}_m$  complexes ( $n, m = 1-4$ ,  $m = n, n + 1$ ) by exploiting an all electron gradient-corrected DFT. The size-dependent binding energy and stability, electronic structure (HOMO–LUMO gap and ioniza-

\* To whom correspondence should be addressed. E-mail: jlwang@seu.edu.cn.

**TABLE 1: Comparison of All-Electron DFT Results (BLYP/DNP) with Experimental (EXP) Studies for Co, Bz, and CoBz Systems<sup>a</sup>**

system	properties	theory	exp <sup>13,36</sup>
Co	IP (eV)	9.06	7.88
Co <sub>2</sub>	R <sub>c</sub> (Å)	2.14	2.31
C <sub>6</sub> H <sub>6</sub>	E <sub>b</sub> (eV)	1.71	1.72
	R <sub>C-C</sub> (Å)	1.40	1.398
	R <sub>C-H</sub> (Å)	1.089	1.084
CoBz	E <sub>b</sub> (eV)	60.99	56.6
	E <sub>b</sub> (eV)	0.22	0.34, 0.64
	IP (eV)	5.648	5.55

<sup>a</sup> R<sub>c</sub> is the equilibrium interatomic distance, IP is the ionization potential, E<sub>b</sub> is the binding energy, for Bz, E<sub>b</sub> = 6E(C) + 6E(H) - E(Bz); for CoBz, E<sub>b</sub> = E(Co) + E(Bz) - E(CoBz).

tion potential), magnetic moments, and coupling nature are also discussed and analyzed.

## II. Computational Methods

In this work, all the calculations are performed at the DFT level using Becke's functional with correlation functional of Lee, Yang, and Parr (BLYP).<sup>37,38</sup> An all electron double numerical basis with polarization functions (DNP) are exploited, as implemented in the DMol package.<sup>39</sup> The self-consistent field calculations are carried out with a convergence criterion of 10<sup>-6</sup> au on the total energy and electron density. Geometry optimizations are performed with the Broyden-Fletcher-Goldfarb-Shanno algorithm. We use a convergence criterion of 10<sup>-3</sup> au on the gradient and displacement and 10<sup>-5</sup> au on the total energy in the geometry optimization. All the structures are optimized without any symmetry constraint. The equilibrium structures are further verified to the true minima from the saddle points of the potential energy surface of the complexes by harmonic frequency computations at a DFT based semi-core pseudopotential basis set (DSPP) as well as a DNP basis set considering the expensive cost of all electron basis set (the equilibrium geometries are first re-optimized at the DSPP level).

The reliability of the BLYP/DNP combination is evaluated by computations on neutrals of Co<sub>n</sub> (n = 1–2), benzene molecule, and CoBz complex. The theoretical and experimental results are presented in Table 1. One can see clearly from the table, the current combination of BLYP/DNP reproduces the measured values well except for isolated Co atom in terms of its ionization energy. Moreover, the current computational scheme identifies similar ground state structures and low-lying energy structures for Co, Co<sub>2</sub>, and CoBz with earlier experiments and theoretical computations.<sup>13,36</sup> Therefore, we can expect that this combination of BLYP/DNP will also give a good description of Co-Bz complexes.

## III. Results and Discussion

The optimized structures of Co<sub>n</sub>Bz<sub>m</sub>, n, m = 1–4, m = n, n + 1 obtained at BLYP/DNP level are displayed in Figure 1–3 and the structure/symmetry, spin-multiplicity, bond length, relative energy, HOMO–LUMO gap of low-lying isomers of the complexes are presented in Table 2.

**A. Geometry. CoBz Complex.** The lowest-energy structure of CoBz is in a doublet state having C<sub>6v</sub> symmetry. The quartet half-sandwich is found to be less stable lying 0.207 eV higher in energy. The binding energy of the Co atom to the benzene molecule in the ground state structure is 0.22 eV, which is in better agreement with the measured values of 0.34<sup>13</sup> and 0.64 eV,<sup>2</sup> than the earlier computational result of 1.83 eV.<sup>13</sup> The cobalt atom lies about 1.415 Å above benzene ring along the

C<sub>6</sub> axis, and the C–C and C–H bond lengths are 1.433 and 1.091 Å in the ground doublet structure, respectively. The quartet state structure has comparable bond lengths for C–C and C–H (only 0.006 and 0.004 Å shorter), but the distance of Co atom to the benzene ring is elongated to 1.629 Å.

**CoBz<sub>2</sub> Complex.** The most stable structure of CoBz<sub>2</sub> is a tilted sandwich in a doublet state, in which the Co atom is located 1.623 Å vertically above one of the benzene rings and about 2.578 Å from the other benzene ring as shown in Figure 1. We should point out that the Co–Bz distance here and in other complexes is defined as the distance of Co atom to the mass center of the benzene ring. The ideal sandwich structure is found to be a transition state with 1.034 eV higher in energy than the ground state. A quartet tilted sandwich structure is found, lying 1.292 eV higher energy than the most stable configuration. However, the negative HOMO–LUMO gap in the quartet state implies it is not a stable solution in term of the wavefunction. Earlier electric deflection,<sup>11</sup> infrared spectroscopy and electron paramagnetic resonance experiments<sup>6</sup> all suggest that CoBz<sub>2</sub> assumes an asymmetric structure. According to 18-electron rule for stable one metal atom compounds, the excess electrons (21 electrons for CoBz<sub>2</sub>) cause the complex distorted to a tilted sandwich structure.<sup>40</sup> That is the reason why CoBz<sub>2</sub> has a structure different from those adopted by early transition metal-benzene clusters like MBz<sub>2</sub>, M = Sc, Ti, V,<sup>17,18,21,28–31</sup> which are perfectly symmetrical sandwich structures.

The binding energy in CoBz<sub>2</sub> of a terminated CoBz to the rest Bz from our computation is 1.667 eV, which is in good agreement with the experimental result (1.71 eV) and much better than the earlier theoretical result (0.42 eV).<sup>13</sup> As compared to CoBz, the C–C and C–H bond lengths in CoBz<sub>2</sub> are not altered significantly, whereas the Co–Bz distances are enlarged about 10% and 80%, respectively.

**Co<sub>2</sub>Bz<sub>2</sub> Complex.** Three initial geometries are considered for geometry optimization: (a) a perpendicular structure in which the Co–Co bond is perpendicular with C<sub>6</sub> axis of benzene ring; (b) a one-end open sandwich structure |•|•, in which Co and Bz are alternatively piled up, (c) a coaxial structure |••|, in which the Co–Co bond is collinear with the C<sub>6</sub> axis of the benzene ring. The optimized structures are displayed in Figure 1. The lowest-energy configuration of Co<sub>2</sub>Bz<sub>2</sub> is found to be a triplet state having a perpendicular structure (C<sub>1</sub>). A similar conformation, but in a singlet state, is nearly degenerate to the ground state structure (ΔE = 0.022 eV) whereas the higher-spin state (quintet) possesses much higher energy (ΔE = 0.791 eV). For the lowest-energy perpendicular structure, both of the Bz molecules are bent and the C–C and C–H bond-lengths are in the ranges 1.377–1.461 and 1.089–1.092 Å, respectively; the distances of Co and the Bz ring are around 2.211–2.478 Å. The Co–Co bond length is 2.428 Å, which is a little longer than that of the bare Co dimer (2.14 Å in this computational scheme).

A distorted one-end-open sandwich structure of triplet multiplicity is localized as an isomer with 0.817 eV higher in energy than the doublet ground state. The “external” Co atom is deviated from the C<sub>6</sub> axis of benzene ring and is bound to two C atoms; the distance of Co to this C–C bond is about 1.909 Å. The middle Bz is significantly distorted and possesses C–C and C–H bond lengths varying from 1.414 to 1.466 and 1.021 to 1.094 Å. The external Bz is almost undistorted with the interior Co atom centered above this Bz by 1.661 Å.

A coaxial structure having D<sub>6h</sub> symmetry is also identified as a local minimum although it possesses much higher energy than the perpendicular ground state. The best coaxial structure

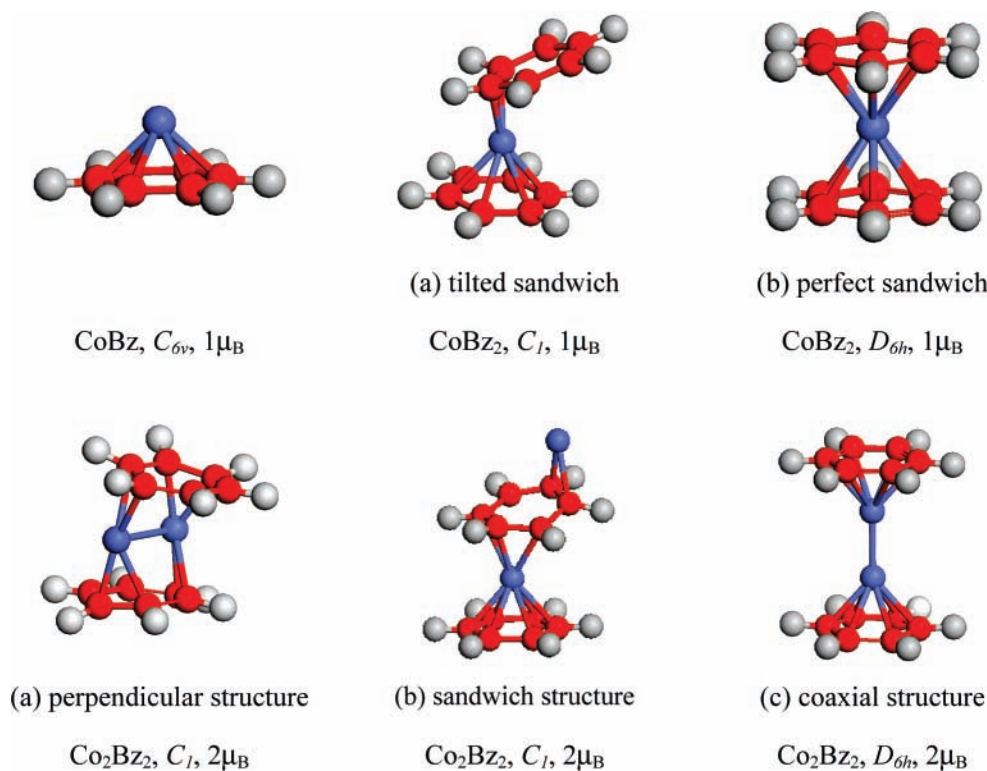


**Figure 1.** Optimized structures of the CoBz, CoBz<sub>2</sub>, and Co<sub>2</sub>Bz<sub>2</sub> complexes.

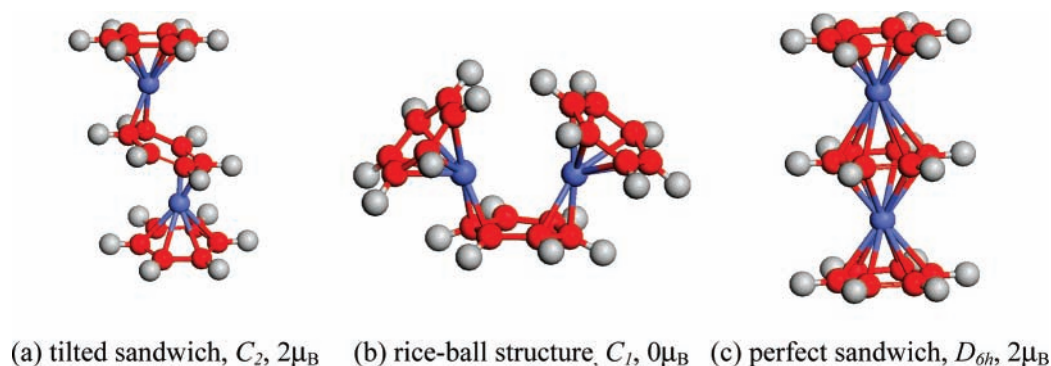


**Figure 2.** Optimized structures of the Co<sub>2</sub>Bz<sub>3</sub> complex.

is in a triplet state and lies 1.041 eV above the lowest-energy perpendicular structure. The singlet and quintet coaxial structures are less stable with 0.018 and 0.194 eV higher in energy than the triplet one. The C–C and C–H bond lengths in this coaxial structure are about 1.421–1.427 and 1.088 Å, and the Co–Bz and Co–Co distances are 1.690 and 2.143 Å. Similar coaxial structure was also identified and the C–C, C–H, Co–Bz, and Co–Co distances are 1.410, 1.09, 1.663, and 1.745 Å in Zhou's calculations.<sup>15</sup>

**Co<sub>2</sub>Bz<sub>3</sub> Complex.** Earlier chemical probe studies<sup>2</sup> suggest the coexistence of both sandwich and rice-ball structures whereas spectroscopic studies<sup>5</sup> suggest the sandwich form for this complex. Therefore, we consider two different structures, sandwich and rice-ball; as initial geometries for geometry optimization and the optimized structures are presented in Figure 2.

**Sandwich Structure.** The equilibrium sandwich structure of Co<sub>2</sub>Bz<sub>3</sub> is very distorted, having  $C_2$  symmetry in which the interior Bz ring is tilted to the external two parallel Bz rings. The perfect sandwich isomer is 2.149 eV higher in energy and possesses nine imaginary frequencies. The most stable sandwich structure is in a triplet state; however, a similar singlet structure

is identified only 0.020 eV higher in energy. The quintet state isomer is much less stable, lying 1.339 eV higher in energy. For the triplet sandwich, the distances of the Co atom to the interior and external Bz rings are about 1.671 and 2.499 Å, respectively, but they are shortened to 1.663 and 2.149 Å in the singlet structure. Similar to the smaller complexes, the C–C and C–H bond lengths in Co<sub>2</sub>Bz<sub>3</sub> sandwiches are insensitive to the spin states of the complexes (cf. Table 2).

**Rice-Ball Structure.** Similar to the sandwich configuration, the optimized rice-ball structure is also quite distorted and lies 0.117 eV above the lowest-energy sandwich structure. The lowest-energy rice-ball structure is in a singlet state and is more stable than the triplet state by 0.069 eV and the quintet state by 0.618 eV in energy. For the lowest-energy singlet structure, the Co–Co bond length is 2.75 Å, much longer than the value of 2.141 Å for the bare Co<sub>2</sub> dimer. One can also note that one of the Bz rings is distorted to a V-shape and the distances of the two Co atoms to this Bz ring are 2.516 and 2.524 Å, respectively. The other two Bz rings have no distortion in shape, interacting singly with one of the Co atoms; the distances of Co–Bz are 1.708 and 1.712 Å, respectively. The Co–Co bond length in the triplet state is practically broken with a very large



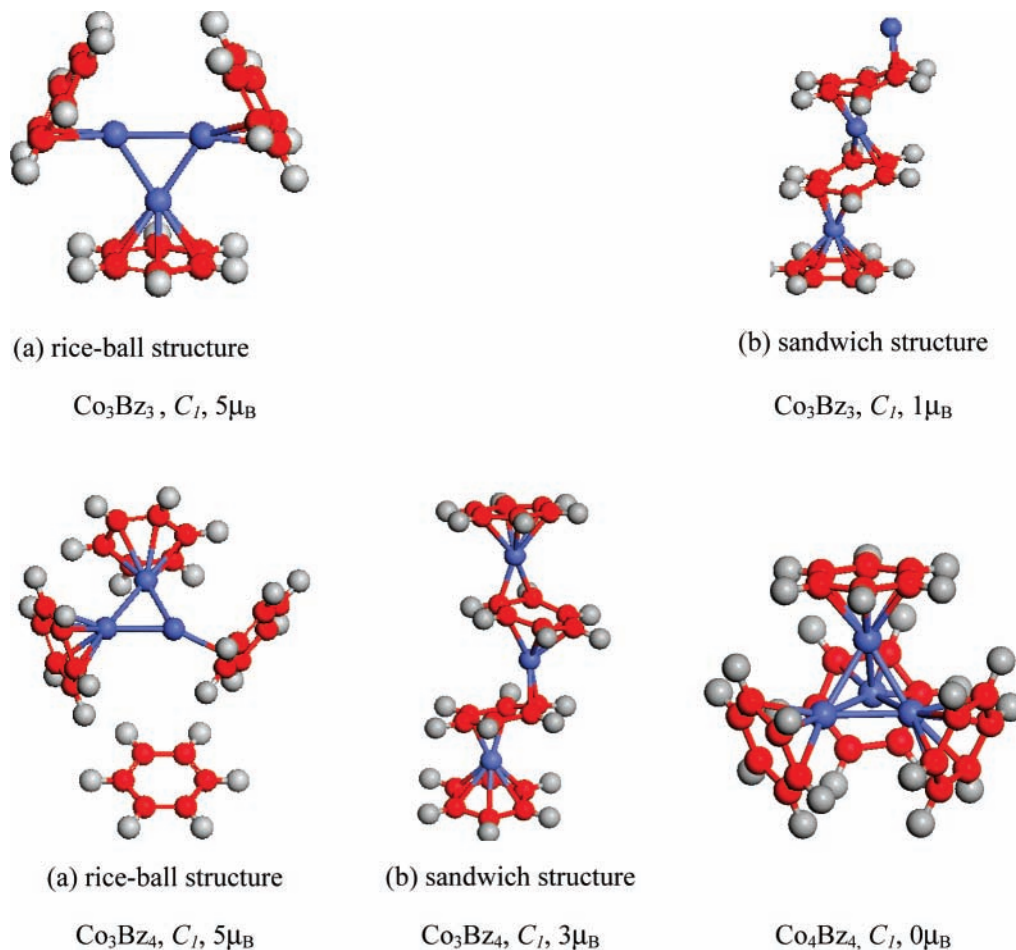


**Figure 3.** Optimized structures of the Co<sub>3</sub>Bz<sub>3</sub>, Co<sub>3</sub>Bz<sub>4</sub>, and Co<sub>4</sub>Bz<sub>4</sub> complexes.

distance of 3.391 Å whereas the other structural parameters such as C–C, C–H, and Co–Bz distances are close to those in the singlet structure.

We should note that the energy difference ( $\Delta E = 0.117$  eV) between the sandwich and rice-ball structures is not big, which implies that the possible coexistence for both of them in the chemical reaction experiments. Therefore, it is reasonable to propose possible reaction mechanisms as (a) benzene molecules reacting with Co<sub>2</sub> clusters (rice-ball structure) and (b) benzene molecules reacting sequentially with Co atoms (sandwich conformation).<sup>2</sup> However, for photoelectron spectroscopy, the well resolving ability might be able to distinguish these two isomers such that only the lowest-energy isomer, the sandwich structure, is thus measured in the spectroscopic study.<sup>5</sup>

**Co<sub>3</sub>Bz<sub>3</sub> Complex.** For the case of Co<sub>3</sub>Bz<sub>3</sub>, chemical probe<sup>2</sup> and spectroscopic studies<sup>5</sup> suggest totally different structures: the former method supports a rice-ball structure based on the fact that there is no reaction with NH<sub>3</sub> (known to attach to uncoordinated metal atoms) and the latter method proposes a sandwich structure for which the most prominent cobalt atomic-like features are observed in the photodetachment spectrum of the Co<sub>3</sub>Bz<sub>3</sub> anion. Therefore, two different structures, a rice-ball structure in which three Co atoms are covered by three Bz rings and a sandwich structure  $|\cdot|\cdot|\cdot$  are both considered as the initial geometries for geometry optimization. The optimized structures are plotted in Figure 3. The lowest-energy structure is a rice-ball structure in a sextet state with the three Co atoms forming an isosceles triangle and Co–Co bond lengths of 2.388 and 2.403 Å, respectively. The distances of Co atom to the

nearest Bz ring are 1.732, 1.738, and 2.851 Å, and the C–C bond lengths vary in the range 1.407–1.422 Å. A doublet rice-ball structure lies 0.058 eV higher in energy than the sextet state, whereas the quartet state is much less stable, lying 0.205 eV higher. The C–C and C–H bond lengths are insensitive to the spin states, whereas Co–Bz distances of the lower-spin states are elongated and their Co–Co bond lengths are shortened slightly as compared with the ground sextet state.

The lowest-energy sandwich structure of (3, 3) is quite distorted and is 1.721 eV higher in energy than that of the rice-ball structure. Therefore, our calculations support the conclusion obtained from chemical probe studies which rice-ball structure is proposed.<sup>2</sup>

**Co<sub>3</sub>Bz<sub>4</sub> Complex.** Similar to Co<sub>2</sub>Bz<sub>3</sub> and Co<sub>3</sub>Bz<sub>3</sub>, both sandwich and rice-ball structures are considered as initial geometries for geometry optimization for the case of Co<sub>3</sub>Bz<sub>4</sub>. The initial rice-ball structure is constructed on the basis of Co<sub>3</sub>Bz<sub>3</sub> by adding an additional Bz molecule and has the C<sub>2v</sub> symmetry. The starting sandwich structure is a perfect structure having D<sub>6h</sub> symmetry. The equilibrium structures are presented in Figure 3.

The lowest-energy structure of Co<sub>3</sub>Bz<sub>4</sub> is a distorted rice-ball motif in a sextet state with C<sub>1</sub> symmetry. In this rice-ball structure, three Co atoms form a scalene triangle with Co–Co bond lengths of 2.306, 2.315, and 2.568 Å. Three of four Bz rings are attached Co atoms, forming a Co<sub>3</sub>Bz<sub>3</sub> core–shell substructure; the distances of Co atom to the Bz molecule are about 1.734, 1.737, and 2.872 Å, respectively. The fourth Bz ring is further away from the frame of Co<sub>3</sub>Bz<sub>3</sub> subunit with a

**TABLE 2: Point Group Symmetry (PGS), Spin-Multiplicities (M), Relative Energies with Respect to the Lowest-Energy Structures ( $\Delta E$ ), Bond Lengths of C–C ( $R_{C-C}$ ), C–H ( $R_{C-H}$ ), and the Distance of the Co Atom to the Mass Center of the Bz Molecule ( $R_{Co-Bz}$ ), HOMO–LUMO Gap ( $\Delta$ ) of the Co–Bz Complexes at the BLYP/DNP Level**

system	PGS	M	$\Delta E$ (eV)	$\Delta$ (eV)	$R_{C-C}$ (Å)	$R_{C-H}$ (Å)	$R_{Co-Bz}$ (Å)	$R_{Co-Co}$ (Å)
CoBz	$C_{6v}$	2	0	0.795	1.433	1.091	1.415	
	$C_{6v}$	4	0.207	0.303	1.421	1.087	1.629	
CoBz <sub>2</sub>	sand- $C_1$	2	0	1.148	1.421–1.423	1.091	1.623, 2.578	
	sand- $C_1$	4	1.292	–0.295 <sup>a</sup>	1.379–1.459	1.090–1.091	2.263, 2.498	2.428
Co <sub>2</sub> Bz <sub>2</sub>	per- $C_1$	3	0	0.943	1.377–1.461	1.089–1.092	2.211–2.478	2.309
	per- $C_1$	1	0.022	1.075	1.368–1.465	1.089–1.093	2.265–2.974	2.513
	per- $C_1$	5	0.791	–0.099 <sup>a</sup>	1.391–1.480	1.089–1.094	2.28–2.515	
	sand- $C_1$	3	0.817	1.209	1.414–1.446	1.043–1.092	1.661–2.478	
	sand- $C_1$	5	1.356	0.282	1.389–1.460	1.088–1.092	1.679–2.605	
	col- $D_{6h}$	3	1.041	0.489	1.421–1.427	1.088–1.089	1.690	2.143
	col- $D_{6h}$	1	1.059	0.491	1.420–1.427	1.088	1.670	2.142
	col- $D_{6h}$	5	1.235	0.581	1.423	1.088–1.089	1.743	2.146
Co <sub>2</sub> Bz <sub>3</sub>	sand- $C_2$	3	0	1.256	1.421–1.476	1.087–1.091	1.671, 2.499	
	sand- $C_2$	1	0.020	1.206	1.418–1.483	1.088–1.092	1.663, 2.199	
	sand- $C_2$	5	1.339	–0.042 <sup>a</sup>	1.390–1.485	1.088–1.091	2.402, 2.151	
	rice- $C_1$	1	0.117	1.201	1.369–1.455	1.086–1.092	1.708–2.524	2.750
	rice- $C_1$	3	0.186	1.066	1.388–1.472	1.085–1.092	1.694–2.629	3.391
	rice- $C_1$	5	0.735	0.594	1.380–1.453	1.087–1.092	2.135–2.517	2.550
Co <sub>3</sub> Bz <sub>3</sub>	rice- $C_1$	6	0	1.052	1.407–1.422	1.088	1.732–2.851	2.312, 2.315, 2.571
	rice- $C_1$	2	0.058	1.053	1.418–1.419	1.088	1.756–1.774	2.388, 2.389, 2.403
	rice- $C_1$	4	0.205	0.630	1.401–1.425	1.088	1.716–3.079	2.298, 2.299, 2.311
	sand- $C_1$	2	1.721	0.274	1.417–1.478	1.088–1.095	1.649–2.453	
	sand- $C_1$	6	1.993	0.960	1.415–1.59	1.088–1.091	1.672–2.748	
	rice- $C_1$	6	0	1.018	1.395–1.423	1.088–1.090	1.734–2.872	2.306, 2.315, 2.568
Co <sub>3</sub> Bz <sub>4</sub>	rice- $C_1$	2	0.049	1.028	1.402–1.421	1.087–1.090	1.756–1.772	2.384, 2.392, 2.401
	rice- $C_1$	4	0.482	0.643	1.402–1.421	1.088–1.090	1.756–1.791	2.379, 2.369, 2.408
	sand- $C_1$	4	0.567	0.819	1.380–1.475	1.089–1.091	1.666–2.519	
	sand- $C_1$	2	0.594	0.771	1.382–1.475	1.088–1.092	1.670–2.535	
	sand- $C_1$	6	1.512	–0.013 <sup>a</sup>	1.397–1.469	1.088–1.092	1.682–2.606	
	rice- $C_1$	1	0	1.105	1.415–1.421	1.088	1.723–1.779	2.507, 2.394, 2.379, 2.396, 2.463, 2.437
Co <sub>4</sub> Bz <sub>4</sub>	rice- $C_1$	3	0.185	0.804	1.416–1.421	1.087	1.722–2.307	2.363, 2.429, 2.436, 2.437, 2.453, 2.723
	rice- $C_1$	5	0.270	0.805	1.413–1.420	1.088	1.765–1.795	2.358, 2.360, 2.362, 2.575, 2.581, 2.596

<sup>a</sup> Negative gap indicates that spin-multiplicity is not the correct one.

**TABLE 3: Structure, Average Binding Energy per Co Atom ( $E_b$ ), HOMO–LUMO Gap, Vertical Ionization Energy (IP), and Average Magnetic Moment per Co Atom ( $\mu$ /atom) of the Lowest-Energy Structure of  $Co_nBz_m$ ,  $n, m = 1-4$ ,  $m = n, n + 1$  at the BLYP/DNP Level Together with the Measured Data<sup>a</sup>**

system	structure	$E_b$ (eV)	$\Delta$ (eV)	IP (eV)		$\mu$ /atom ( $\mu_B$ )	
				BLYP	exp <sup>2</sup>	BLYP	exp <sup>8</sup>
CoBz	half-sand	0.221	0.795	5.468	5.55 ± 0.04	1.0	
CoBz <sub>2</sub>	sandwich	1.457	1.148	5.614	5.53 ± 0.03	1.0	
Co <sub>2</sub> Bz <sub>2</sub>	per-sand	1.538	0.943	5.353	4.94 ± 0.05	1.0	
Co <sub>2</sub> Bz <sub>3</sub>	sandwich	1.595	1.256	5.107 (4.785)	4.85 ± 0.04(S)	1.0	2.098 ± 0.449
	rice-ball	1.561	1.201	4.98 (5.057)	5.00 ± 0.05(R)	0	
Co <sub>3</sub> Bz <sub>3</sub>	rice-ball	1.762	1.052	4.855 (5.121)	5.16 ± 0.06	1.667	1.039 ± 0.254
Co <sub>3</sub> Bz <sub>4</sub>	rice-ball	1.748	1.018	4.80	4.64 ± 0.05	1.667	1.571 ± 0.300
Co <sub>4</sub> Bz <sub>4</sub>	rice-ball	2.028	1.105	4.387	4.92 ± 0.05	0	0.669 ± 0.122

<sup>a</sup> The data in parentheses are for the low-lying isomers.

distance to all of the Co atoms of about 7.023 Å. Interestingly, the dissociation energy of this rice-ball structure with respect to a relaxed Co<sub>3</sub>Bz<sub>3</sub> core–shell structure and Bz molecule is –0.046 eV, implying that it is spontaneously dissociated to a Co<sub>3</sub>Bz<sub>3</sub> rice-ball unit and a Bz fragment. This might explain why there is no prominent peak at (3, 4) in the time-of-flight mass spectrum.<sup>2</sup>

A similar rice-ball structure, but in a doublet state, is identified as a local minimum having only 0.049 eV higher in energy, whereas the quartet state structure possesses much higher energy ( $\Delta E = 0.482$  eV) as compared to the sextet ground state. These two isomers have bond lengths for C–C, C–H, Co–Bz, and Co–Co similar to those found for the sextet state.

The optimized sandwich structure for Co<sub>3</sub>Bz<sub>4</sub> is significantly distorted with the external two Bz rings being parallel and the internal two Bz rings being tilted; the perfect sandwich structure lies at a much higher energy ( $\Delta E = 3.614$  eV). Unlike the

lowest-energy rice-ball structure, the lowest-energy sandwich structure is in a quartet state, and it is less stable than the best rice-ball structure by 0.567 eV higher in energy. The doublet and sextet sandwiches have 0.027 and 0.945 eV higher in energy as compared to the quartet state. For the quartet sandwich structure, the distances of the Co atoms to Bz rings are 1.670, 2.504, 2.454, 1.728, 2.519, and 1.666 Å from the one end to the other; the C–C and C–H bond lengths are around 1.38–1.48 and 1.09 Å, respectively. The doublet and sextet state structures have similar Co–Bz distances and C–C and C–H bond lengths as that of the quartet state structure.

**Co<sub>4</sub>Bz<sub>4</sub> Complex.** Because both chemical probe and spectroscopic studies suggest rice-ball structure for  $n \geq 4$ , only the rice-ball structure in which four Co atoms forming a tetrahedron covered by four Bz rings is considered. The initial geometry has a high symmetry of  $T_d$ , but geometry optimization leads to a distorted rice-ball without any symmetry elements ( $C_1$ ). The

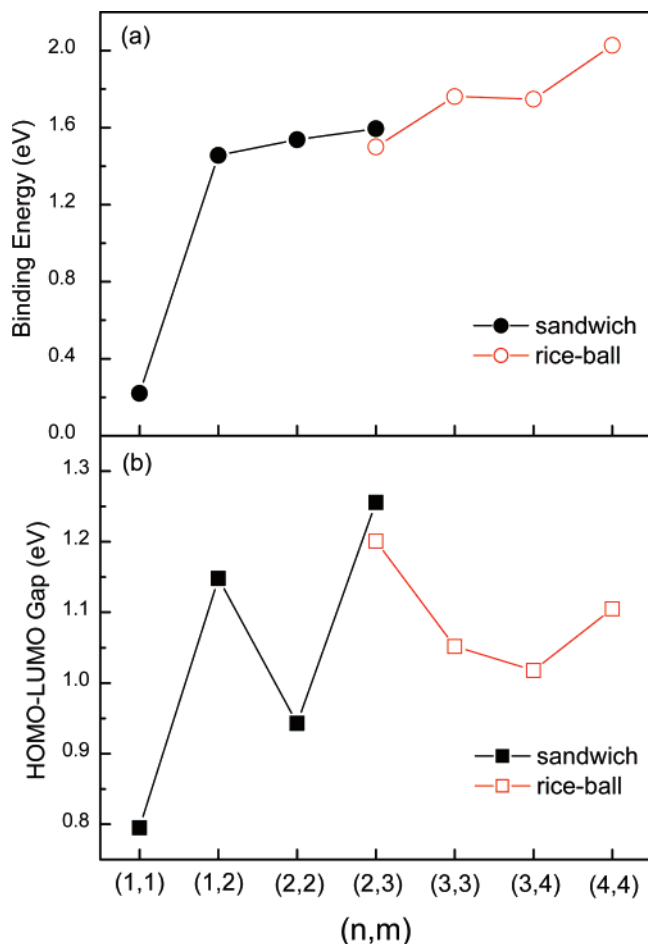


**Figure 4.** (a) Average binding energy per Co atom and (b) the HOMO–LUMO gap of the lowest-energy structures of Co<sub>n</sub>Bz<sub>m</sub>. For the case of (2, 3), both sandwich and rice-ball results are presented.

ground spin state is determined as a singlet state. The distances from each Co atom to the nearest Bz ring are 1.723, 1.734, 1.748, and 1.779 Å and the Co–Co bond lengths are in the range 2.39–2.51 Å, respectively. The higher-spin states of this cluster, triplet and quintet, are less stable lying 0.185 and 0.270 eV higher in energy. The C–C, C–H, and Co–Co bond lengths and the Co–Bz distances are relatively insensitive to the spin states, with values of 1.42, 1.09, 2.36–2.73, and 1.72–1.79 Å, respectively.

**B. Size-Dependent Energetic, Electronic, and Magnetic Properties.** The structure, the binding energy, the HOMO–LUMO gap, and the vertical ionization energy of the lowest-energy structures of Co<sub>n</sub>Bz<sub>m</sub>,  $n, m = 1–4, m = n, n + 1$  at the BLYP/DNP level are presented in Table 3 together with the measured data.

**Binding Energy.** The average binding energy (BE( $n, m$ )) per Co atom of a Co<sub>n</sub>Bz<sub>m</sub> complex with respect to individual Co atom and Bz ring is computed using the following equation,

$$BE(n, m) = \{nE[\text{Co}] + mE[\text{Bz}] - E[\text{Co}_n\text{Bz}_m]\}/n$$

in which the  $E[\cdot]$  are the total energy of the relaxed Co<sub>n</sub>Bz<sub>m</sub>, Bz molecule, and isolated Co atom.

As displayed in Figure 4a, the average binding energy of the Co–Bz complexes increases rapidly from 0.221 eV of the CoBz half sandwich to 1.457 eV of the smallest full (tilted) sandwich CoBz<sub>2</sub> then increases gradually as increasing with cluster size afterward. The BE( $n, m$ ) curve reaches local maxima at (3, 3) and (4, 4) indicating that these clusters are more stable than

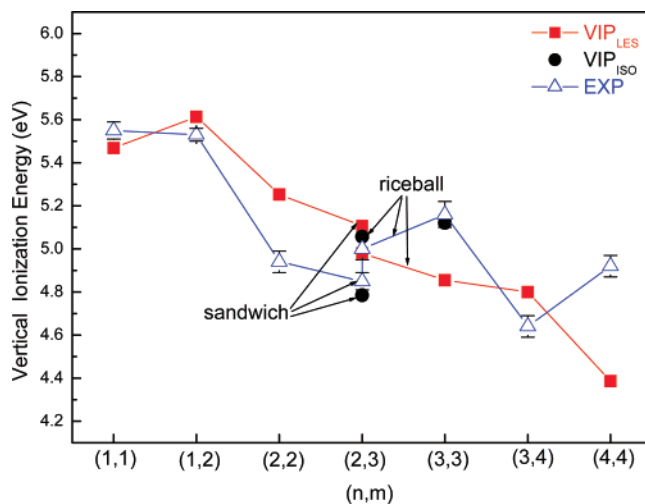


**Figure 5.** Computed and measured ionization potentials of the lowest-energy structures (VIP<sub>LES</sub>), the second low-lying isomer (VIP<sub>ISO</sub>) and the measured data (EXP)<sup>2</sup> of Co<sub>n</sub>Bz<sub>m</sub>. For the case of (2, 3), both sandwich and rice-ball results are presented.

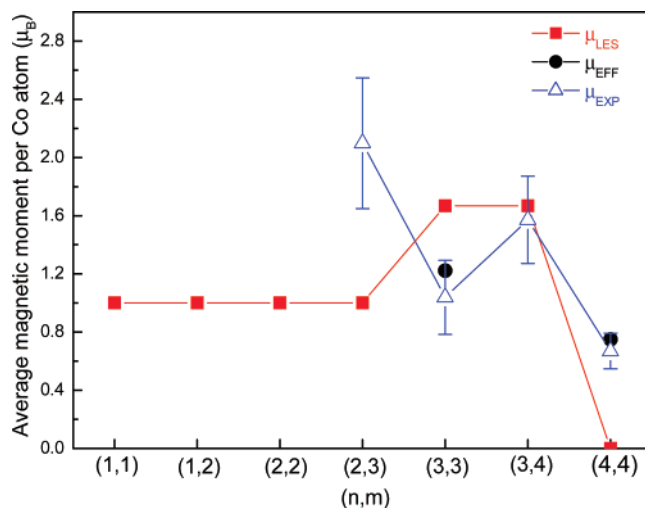


**Figure 6.** Computed magnetic moments of the lowest-energy structure ( $\mu_{\text{LES}}$ ), the effective magnetic moment ( $\mu_{\text{EFF}}$ ), and the measured data ( $\mu_{\text{EXP}}$ )<sup>8</sup> per Co atom as functions of cluster size.

**TABLE 4: Total Magnetic Moment ( $\mu$ ), Relative Energy ( $\Delta E$ ), Average Magnetic Moment of Low-Lying Isomers ( $\mu/\text{atom}$ ), Effective Average Magnetic Moment ( $\mu_{\text{eff}}/\text{atom}$ ) and Measured Magnetic Moment ( $\mu_{\text{exp}}$ ) per Co Atom for the (3, 3) and (4, 4) Clusters**

system	$\mu$ ( $\mu_{\text{B}}$ )	$\Delta E$ (eV)	$\mu/\text{atom}$ ( $\mu_{\text{B}}$ )	$\mu_{\text{eff}}/\text{atom}$ ( $\mu_{\text{B}}$ )	$\mu_{\text{exp}}/\text{atom}^8$ ( $\mu_{\text{B}}$ )
Co <sub>3</sub> Bz <sub>3</sub>	5	0	1.667	1.222	1.039 ± 0.254
	1	0.058	0.333	-	-
	3	0.205	1.0	-	-
Co <sub>4</sub> Bz <sub>4</sub>	0	0	0	0.75	0.669 ± 0.122
	2	0.185	0.500	-	-
	4	0.270	1.0	-	-

others such as (2, 3) and (3, 4). This is easy to understand because each Bz ring is attached one Co atom for ( $n, n$ ) cases whereas for ( $n, n + 1$ ) one of the Bz rings is unbound to the Co atom and the binding energy is thus smaller. Moreover, as clearly seen from the figure, the sandwich structure competes with the rice-ball conformation at the composition (2, 3), which explains the coexistence of the sandwich and rice-ball structure as was inferred experimentally.<sup>2</sup>

**HOMO–LUMO Gap.** The HOMO–LUMO gap reflects the kinetic stability of a cluster. The HOMO–LUMO gap of the lowest-energy Co<sub>n</sub>Bz<sub>m</sub> structures is presented as a function of

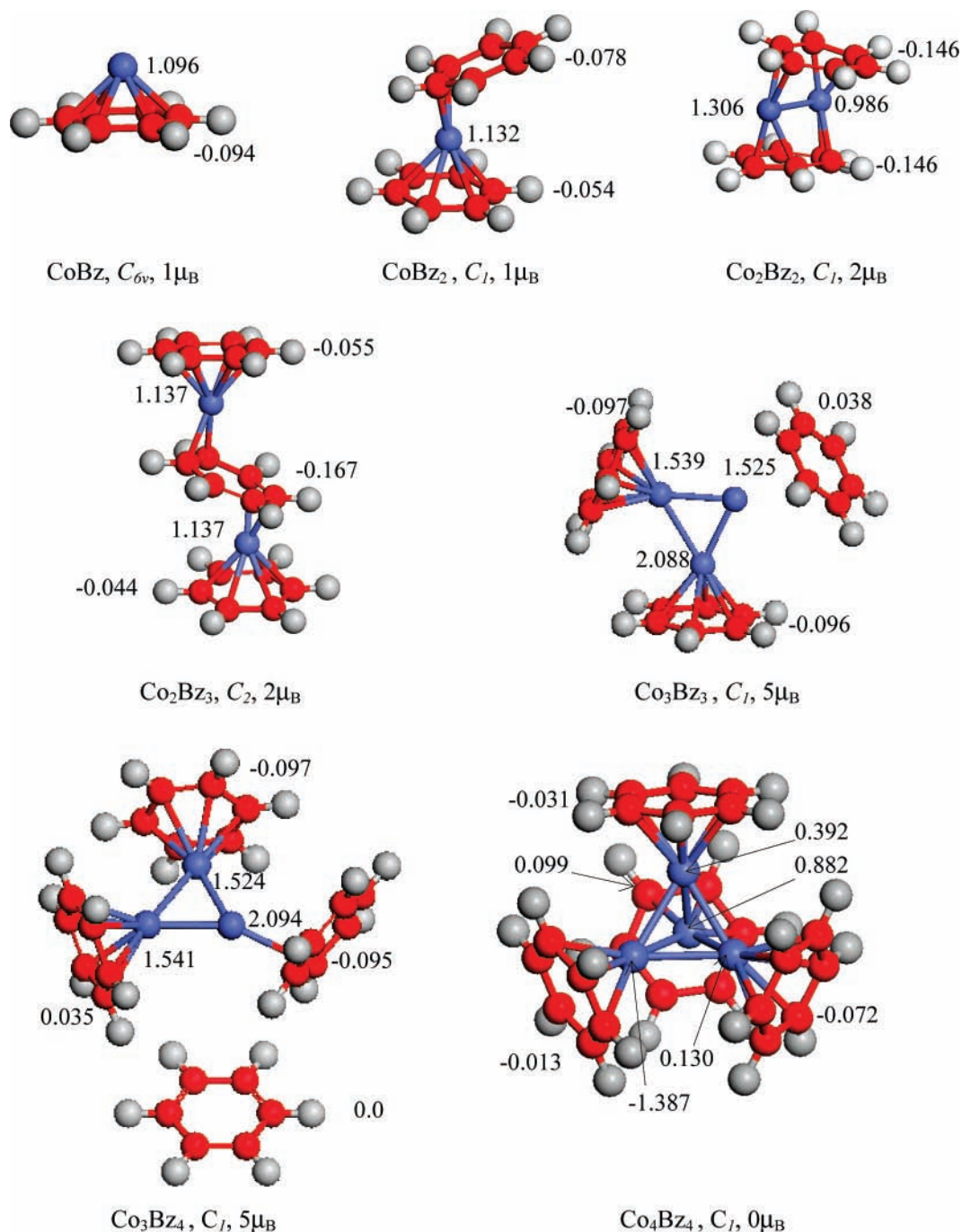


**Figure 7.** Local atomic moment on each Co atom and benzene molecule of the lowest-energy structures of the  $Co_nBz_m$  complexes.

cluster size in Figure 4b. It is interesting to note that the HOMO–LUMO gap curve shows a clear “odd–even” alternative for the smaller sandwich structures with  $n \leq 2$  in which the series of  $(n, n + 1)$ , e.g., (1, 2) and (2, 3), have larger gaps and the  $(n, n)$  clusters, e.g., (1, 1) and (2, 2), have smaller gaps. This infers that the  $(n, n + 1)$  complexes have relatively large kinetic stabilities. In particular, the gap in the (2, 3) sandwich structure is larger than that in the rice-ball, which also implies that the sandwich structure is more stable than the rice-ball structure. On the contrary, for the larger rice-ball clusters for  $n \geq 3$ , the  $(n, n)$  series of (3, 3) and (4, 4) have gaps relatively larger than  $(n, n + 1)$  of (3, 4), which has the similar tendency of the average binding energy.

Note that the values of the HOMO–LUMO gaps of all the Co–Bz complexes studied here (Table 3) are of significant

magnitude, which suggests that these complexes are quite stable regardless if they are in sandwich or rice-ball form.

**Ionization Potential.** The ionization potential (IP) is the energy required to remove one electron from a cluster and can be measured relatively easily experimentally. In this study, the vertical ionization potentials (VIPs) of the lowest-energy Co–Bz complexes are calculated (Table 3 and Figure 5). Because the IPs of sandwich and rice-ball structures were measured for Co<sub>2</sub>Bz<sub>3</sub>, both VIP of these two conformations are also computed here. As shown in Figure 5, our prediction of the VIP is overall in good accord with the measured results,<sup>2</sup> with discrepancies of less than 0.3 eV for all the sizes except the (4, 4) case. Furthermore, we note that the VIP of the second lowest-energy isomer reproduces the measured data better for the cases of (2, 3), (3, 3). This is not difficult to understand because the



computed energies of these isomers lie only slightly above the ground state structure and might contribute to the photoionization spectrum, in which case the measured IP may be actually an average of all these close-energy isomers.

We should point out that earlier DFT computations<sup>13</sup> also explored the VIP and the value that was found is much smaller than the measured one.<sup>2</sup> The large discrepancy might come from the fact that in this prior study, the structure of CoBz<sub>2</sub> was constrained to be a perfect sandwich structure with *D*<sub>6h</sub> symmetry.

**Magnetic Properties.** From our calculations, the average magnetic moment per Co atom remains a constant as 1 μ<sub>B</sub> for the smaller complexes of (1, 1), (1, 2), and (2, 2). The common feature of these complexes is that they all have sandwich conformations, which implies that each Co atom contributes about 1 μ<sub>B</sub> to the complexes. For the case of (3, 3) and (3, 4), much larger moments, as high as 1.677 μ<sub>B</sub>/atom, are obtained whereas a zero moment is obtained for (4, 4). Compared with recent Stern–Gerlach deflection experiments, the computed moments in this approach are in good agreement with the measured value at (3, 4), but large discrepancies are found for (2, 3), (3, 3), and (4, 4).

From the discussions above, we have identified a few close-energy isomers for a given cluster. For example, for the case of (3, 3), the low-spin doublet state is degenerated to the sextet ground state with the energy difference of only 0.058 eV. Similarly, the higher-spin states of triplet and quintet of Co<sub>4</sub>Bz<sub>4</sub> are less stable than the singlet state by only 0.185 and 0.270 eV higher in energy. The presence of several energetically close isomers may not be distinguished in Stern–Gerlach deflection experiments due to the limited resolving ability of the experimental apparatus. Thus, the measured moment might be a mixture of these close-energy isomers, and the “effective” magnetic moment, which is a spin-weighted average over the quasi-degenerate structures, should be a more reasonable benchmark to compare to the experiment. In our previous work on vanadium–benzene sandwich clusters,<sup>28</sup> the measured moments were well reproduced as the “effective” magnetic moments  $\bar{S}$ , defined as

$$\bar{S} = \frac{\sum_i (2S_i + 1)S_i}{\sum_i (2S_i + 1)} \quad (1)$$

where *S<sub>i</sub>* is the total magnetic moment of the *i*th low-lying isomer in spin. We present the average moments of the lowest-energy structures and the second (third) isomers with nearly degenerate energies, the “effective” magnetic moments through eq 1 together with the measured values in Table 4 and Figure 6. One can see it clearly from Table 4 that the measured moment lies between the values of the lowest-energy structures and the alternative low-lying isomers for (3, 3) and (4, 4). The effective magnetic moment matches the measured ones very well. This indicates the measured moment is actually a mixture of a few close-energy isomers having different spin states. However, the failure at (2, 3) between the computed and measured moment remains unexplained, which might stem from the coexistence of both sandwich and rice-ball structures. Another possible reason might be due to the fact that DFT computes structures in their static states (0 K) whereas the experimental moment is measured at finite temperature (58 ± 2 K).<sup>8</sup> This suggests that further computations and measurements are needed to verify and understand the magnetism of Co<sub>2</sub>Bz<sub>3</sub>.

To further illustrate the magnetic nature of the Co<sub>n</sub>Bz<sub>m</sub> complexes, we present the local atomic moment on each Co atom and Bz molecule obtained by Mulliken population analysis in Figure 7. First, the magnetism of the complexes mostly stems from the contribution of Co atoms and most of the local atomic moments are more than 1.0 μ<sub>B</sub>; very small moments (less than 0.15 μ<sub>B</sub>) are found on Bz molecules with opposite spin direction. Second, for the sandwich forms, each Co atom possesses about 1 μ<sub>B</sub> moment; however, it has much larger values (≥ 1.5 μ<sub>B</sub>) for rice-ball structures of (3, 3) and (3, 4). Third, ferromagnetic alignment/ferromagnetic ordering (where all the spins on Co atoms are parallel) is favored for the smaller compositions up to (3, 4), whereas antiferromagnetic/ferrimagnetic alignment is observed for the largest cluster of (4, 4). In the case of (4, 4), one of Co atoms possesses a relatively large negative moment of 1.387 μ<sub>B</sub> (spin-down), and three other Co atoms have 0.13, 0.392, and 0.882 μ<sub>B</sub> moments (spin-up), respectively. In the triplet state of (4, 4), two of the Co atoms are antiparallel to two other Co atoms with the atomic moment of 1.530 and 1.534 vs −0.420 and −0.521 μ<sub>B</sub>. For its quintet state, four Co atoms are ferromagnetically aligned with atomic moments of 0.824, 0.827, 0.897, and 1.680 μ<sub>B</sub>, respectively. The energetically favorite antiferromagnetic/ferrimagnetic ordering of Co atoms quenches the magnetism of the (4, 4) complex.

To compare to bare Co clusters, we performed similar DFT computations on Co<sub>2–4</sub> clusters and the average magnetic moments per atom are 2.5, 2.133, and 2.5 μ<sub>B</sub>, respectively. These computed moments are consistent with the experimental estimates<sup>41</sup> (more than 2.0 μ<sub>B</sub>/atom), which again justifies our computational approach. Apparently, the magnetic moments in Bz-based cobalt clusters (≤ 1.667 per Co atom) are reduced when Co clusters are in Bz matrix, indicating that Bz molecules play a quenching role to the magnetism of the Co–Bz complexes.

#### IV. Conclusion

We have carried out all electronic density functional theory calculations on the Co<sub>n</sub>Bz<sub>m</sub>, *n* = 1–4, *m* = *n*, *n* + 1, complexes. The size- and composition-dependent structural, electronic, and magnetic properties of the complexes have been investigated. Sandwich conformations are energetically preferred for the smallest size; rice-ball structures are favored for larger sizes with *n* ≥ 3. Both sandwich structure and rice-ball structure are identified, coexisting for Co<sub>2</sub>Bz<sub>3</sub>, and the former is more stable in terms of binding energy and HOMO–LUMO gap. The binding energy increases rapidly from the half-sandwich to the tilted full sandwich and is relative larger at rice-ball clusters of (3, 3) and (4, 4). Large HOMO–LUMO gaps are found for all the compositions studied here, and smaller sandwich at (*n*, *n*+1) and larger rice-ball at (*n*, *n*) clusters have highly kinetic stability. The computed ionization energy and magnetic moments of Co<sub>n</sub>Bz<sub>m</sub> clusters are in good agreement with the measured results overall, and the measured ones are a mixture of a few low-lying isomers with different spin states. Ferromagnetic alignment of Co atoms is energetically preferred for smaller complexes with *n* = 1–3 and *m* = *n*, *n* + 1 and antiferromagnetic/ferrimagnetic ordering is favored for the (4, 4) composition. The reduced magnetic moments in Co–Bz complexes indicate that absorption of Bz molecules quenches the magnetism of the Co clusters.

**Acknowledgment.** The work is supported by the National Nature Science Foundation of China (No. 10604013), the Program for New Century Excellent Talents in the University



of China (NCET-06-0470), Qinglan Project in the University of Jiangsu Province, and the Teaching and Research Foundation for the Outstanding Young Faculty of Southeast University. J.W. thanks Dr. M. B. Knickelbein for valuable discussions. We thank the computational resource at Nanjing University.

### References and Notes

- (1) Long, N. J. *Metalloenes*; Blackwell Science: Oxford, U.K., 1998.
- (2) Kurikawa, T.; Hirano, M.; Takeda, H.; Yagi, K.; Hoshino, K.; Nakajima, A.; Kaya, K. *J. Phys. Chem.* **1995**, *99*, 16248.
- (3) Kurikawa, T.; Takeda, H.; Hirano, M.; Judai, K.; Arita, T.; Nagao, S.; Nakajima, A.; Kaya, K. *Organometallics* **1999**, *18*, 1430.
- (4) Nakajima, A.; Kaya, K. *J. Phys. Chem. A* **2000**, *104*, 176.
- (5) Gerhards, M.; Thomas, O. C.; Nilles, J. M.; Zheng, W. J.; Bowen, K. H., Jr. *J. Chem. Phys.* **2002**, *116*, 23.
- (6) Bechamp, K.; Levesque, M.; Joly, H.; Manceron, L. *J. Phys. Chem. A* **2006**, *110*, 6023.
- (7) Jaeger, T. D.; Heijnsbergen, D. V.; Klippenstein, S. J.; Helden, G.; Meijer, G.; Duncan, M. A. *J. Am. Chem. Soc.* **2004**, *126*, 10981.
- (8) Knickelbein, M. B. *J. Chem. Phys.* **2006**, *125*, 044308.
- (9) Chaquin, P.; Costa, D.; Lepetit, C.; Che, M. *J. Phys. Chem. A* **2001**, *105*, 4541.
- (10) Bauschlicher, C. W., Jr.; Partridge, H.; Langhoff, S. R. *J. Phys. Chem.* **1992**, *96*, 3273.
- (11) Rayane, D.; Allouche, A. R.; Antoine, R.; Broyer, M.; Compagnon, I.; Dugourd, P. *Chem. Phys. Lett.* **2003**, *375*, 506.
- (12) Meyer, F.; Khan, F. A.; Armentrout, P. B. *J. Am. Chem. Soc.* **1995**, *117*, 9740.
- (13) Pandey, R.; Rao, B. K.; P. Jena.; Blanco, M. A. *J. Am. Chem. Soc.* **2001**, *123*, 3799.
- (14) Yang, C. N.; Klippenstein, S. J. *J. Phys. Chem. A* **1999**, *103*, 1094.
- (15) Zhou, J.; Wang, W. N.; Fan, K. N. *Chem. Phys. Lett.* **2006**, *424*, 247.
- (16) Pandey, R.; Rao, B. K.; Jena, P.; Newsam, J. M. *Chem. Phys. Lett.* **2000**, *321*, 142.
- (17) Sohnlein, B. R.; Li, S. G.; Yang, D. S. *J. Chem. Phys.* **2005**, *123*, 214306.
- (18) Zheng, W. J.; Nilles, J. M.; Thomas, O. C.; Bowen, K. H., Jr. *Chem. Phys. Lett.* **2005**, *401*, 266.
- (19) Cloke, F. G. N.; Dix, A. N.; Green, J. C.; Perutz, R. N.; Seddon, E. A. *Organometallics* **1983**, *2*, 1150.
- (20) Nagaoka, S.; Matsumoto, T.; Ikemoto, K.; Mitsui, M.; Nakajima, A. *J. Am. Chem. Soc.* **2007**, *129*, 1528.
- (21) Weis, P.; Kemper, P. R.; Bowers, M. T. *J. Phys. Chem. A* **1997**, *101*, 8207.
- (22) Zakin, M. R.; Cox, D. M.; Brickman, R. O.; Kaldor, A. *J. Phys. Chem.* **1989**, *93*, 18.
- (23) Andrews, M. P.; Mattar, S. M.; Ozin, G. A. *J. Phys. Chem.* **1986**, *90*, 744.
- (24) Miyajima, K.; Yabushita, S.; Knickelbein, M. B.; Nakajima, A. *J. Am. Chem. Soc.* **2007**, *129*, 8473.
- (25) Miyajima, K.; Nakajima, A.; Yabushita, S.; Knickelbein, M. B.; Kaya, K. *J. Am. Chem. Soc.* **2004**, *126*, 13202.
- (26) Maslyuk, V. V.; Bagrets, A.; Meded, V.; Arnold, A.; Evers, F.; Brandbyge, M.; Bredow, T.; Mertig, I. *Phys. Rev. Lett.* **2006**, *97*, 097201.
- (27) Xiang, H. J.; Yang, J. L.; Hou, J. G.; Zhu, Q. S. *J. Am. Chem. Soc.* **2006**, *128*, 2310.
- (28) Wang, J.; Acioli, P. H.; Jellinek, J. *J. Am. Chem. Soc.* **2005**, *127*, 2812.
- (29) Wang, J.; Jellinek, J. *J. Phys. Chem. A* **2005**, *109*, 10180.
- (30) Kandalam, A. K.; Rao, B. K.; Jena, P.; Pandey, R. *J. Chem. Phys.* **2004**, *120*, 10414.
- (31) Kua, J.; Tomlin, K. M. *J. Phys. Chem. A* **2006**, *110*, 11988.
- (32) Yasuike, T.; Nakajima, A.; Yabushita, S.; Kaya, K. *J. Phys. Chem. A* **1997**, *101*, 5360.
- (33) Yasuike, T.; Yabushita, S. *J. Phys. Chem. A* **1999**, *103*, 4533.
- (34) Ouhlal, A.; Selmani, A.; Yelon, A. *Chem. Phys. Lett.* **1995**, *243*, 269.
- (35) Rabilloud, F. *J. Chem. Phys.* **2005**, *122*, 134303.
- (36) Kaut, A.; Strauss, B. *J. Chem. Phys.* **1964**, *41*, 3806.
- (37) Becke, A. D. *J. Chem. Phys.* **1988**, *88*, 2547.
- (38) Lee, C.; Yang, W.; Parr, R. G. *Phys. Rev. B* **1988**, *37*, 785.
- (39) DMOL is a density functional theory program distributed by Accelrys, Inc. Delley, B. *J. Chem. Phys.* **1990**, *92*, 508; *J. Chem. Phys.* **2000**, *113*, 7756.
- (40) Lauher, J. W.; Elian, M.; Summerville, R. H.; Hoffmann, R. *J. Am. Chem. Soc.* **1976**, *98*, 3219.
- (41) Xu, X. S.; Yin, S. Y.; Moro, R.; de Heer, W. A. *Phys. Rev. Lett.* **2005**, *95*, 237209.